PALMS
(Pacific Area Longevity Medical Society)

No.13 Journal
(October 2017)

- Let's save many lives in Pacific Area each other all together enhancing our medical skill on the skill-depended discussion collaborating each other.

- The Chair Area will be turned Clockwise Starting from Micronesia to Polynesia, and to then Melanesia by 3 years as the repeated sequence. It'll come to your place

The present H.Q. (Head Quarter) of PALMS

c/o New Tokyo Medical College
1, Kapwar E Sou, Kolonia, Pohnpei States
Federated States of Micronesia (Micronesia Area)
Tel: +691-320-3815 or +691-920-2977
Fax: +691-320-3391
http://www.geocities.jp/rainbow_8092/PALMS.html
E-mail: okada@ntmc.fm or rainbow_vc@yahoo.co.jp

Journal of Pacific Area Longevity Medical Society (PALMS) published on October 2017 to All Pacific from Kolonia, Pohnpei, the Federated States of Micronesia
<PALMS: Established in Sep 1st in 2016 on the consultation between Micronesia, Polynesia, and Melanesia>

11 . Remote Measurement of Pulse Transit Time

Based on Fluctuation of Hemoglobin Component

Munenori Fukunishi, Taku Yonezawa, Genki Okada, Kouki Kurita, *Chiba University,*
Shoji Yamamoto, *Tokyo Metropolitan College of Industrial Technology*,
Norimichi Tsumura, *Chiba University*

*(Ja*pan: *fukunish.m@gmail.com, tsumura@faculty.chiba-u.jp)*

Field :LL

***Abstract*— Blood pressure is, in most of case, measured with a contact device called a sphygmomanometer cuff. Recently blood pressure can be easily measured with portable devices such as smart watches that take advantage of the progress of mobile technology. Even with the use of mobile devices, contact measurement is still required, which could be one of the mandatory conditions for healthcare applications. In this paper, we propose the remote video based estimation of pulse transit time (PTT) based on the quantification method of hemoglobin level. We confirm high correlation between PTT measured by the proposed method and the blood pressure measurement with sphygmomanometer cuff, whose R, correlation coefficient, is between -0.5792 to -0.7801.**

***Index Terms*— Pulse Transit Time, Blood Pressure, Non-Con tact Measurement**

I. Introduction

Vital signs are the most basic measurements of the body's functions. Vital signs typically include the measurement of: body temperature, respiration rate, pulse rate, blood pressure. Blood pressure is related to the functional status of heart and blood vessels. The measurement is crucial to detect hypertension, to prevent, control and follow up them. In most cases, it is measured with sphygmomanometer cuff, which requires the subject to remain still. It restricts the frequency and convenience of usage.

With recent advances in mobile technology, some of the remote vital sign measurements are already in practical use or have been studied for several years. For example, infrared thermometer can detect body temperature remotely and commercially available [1-3]. Aoki et al. [4] proposed a non-contact respiration measurement technique, using the firstgeneration Kinect, by extracting the volume of the thoracoabdominal region using the skeleton joint positions available from the sensor. Poh et al. [5,6] developed the remote measurement technique for blood volume pulse (BVP) signal using a low-cost webcam, based on blind source separation and demonstrated the remote measurement of pulse rate. As to blood pressure, OMRON [7] announced the blood pressure measurement using smart watch. However it still requires contact measurement, which limits application from a wide variety of use cases. In order to expand the usage, remote measurement of blood pressure is significant. However it is still in research stage. It is known that

blood pressure can be estimated by the detection of Pulse Transit Time (PTT), which is the timing gap between two blood volume pulses at two parts of the body. For the non-contact measurement of PTT, Shao et al. [8] developed non-contact PTT measurement using a conventional camera. Its method measures the brightness of green in the hand and face region and calculates PTT using the delay in the peak times. Murakami at el. [9] measured PTT with the green channel peaks on regions of the hand and ankle, and evaluated the relation between PTT and blood pressure. On the other hand, Tsumura el al. [10] proposed a method to estimate hemoglobin level and blood amount from a biological color image. The method potentially improves the accuracy of estimation of BVP timing since the amount of blood and hemoglobin levels in the blood vessel are correlated with BVP.

In this paper, therefore, we propose a non-contact video based estimation method of pulse transit time (PTT) using the measurement of hemoglobin composition. The proposed method is aimed to obtain PTT accurately only by capturing video remotely.

In section 2, we present how to extract hemoglobin information from a biological color image. In section 3, we describe the experimental setup to obtain BVP and PTT. In section 4 and 5, we describe the experimental results and conclusion, respectively.

Ⅱ. Extraction of Hemoglobin Information from a Biological Color Image

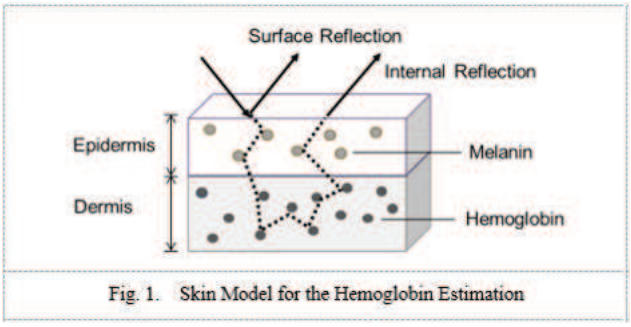

Fig. 1. Skin Model for the Hemoglobin Estimation

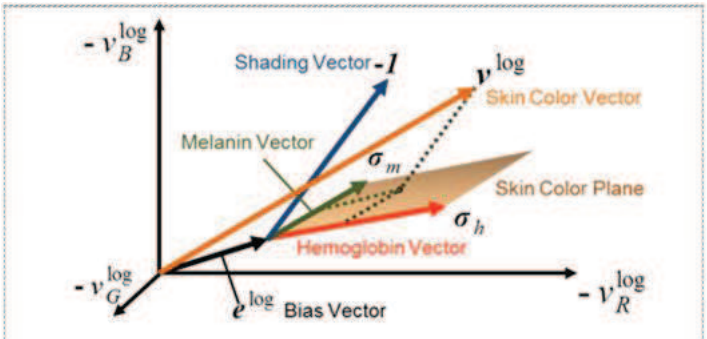

Fig. 2. Model of Observation Signals. Skin color vector v^{log} is logarithmic value of RGB camera signal on skin region. Skin color vector v^{log} consists of Melanin vector σ_m, Hemoglobin vector σ_h and shading vector $\mathbf{1}$. A skin color plane is predefined using training data set. Skin color vector is projected onto the skin color plane along with the shading vector $\mathbf{1}$. From the position on the skin plane, we obtain the amount of hemoglobin vector.

The method to estimate hemoglobin amount per a volume was proposed by Tsumura el al. [10]. The method potentially improves the accuracy of hemoglobin level is correlated with BVP. In this section, we describe the method to extract hemoglobin information.

Figure 1 shows the skin model of hemoglobin level estimation. Human skin can be roughly classified into two layers, epidermis and dermis. Epidermis has melanin pigments, and dermis has hemoglobin pigments. Some of the incident light illuminated onto skin is reflected on the surface as surface reflection. Others go into the epidermis and dermis. In those medium, the light undergoes internal reflection where it bounces randomly and comes to the surface of the skin. In the process of internal reflection, some of the light is absorbed by

the melanin and hemoglobin pigments. The modified Lambert-Beer law [11] is an approximate model of internal light behavior. The spectral radiance $L(x,y,\lambda)$of internal reflection is

$$L(x,y,\lambda) = e^{-\rho_m(x,y)\sigma_m(\lambda)l_e(\lambda)-\rho_h(x,y)\sigma_h(\lambda)l_d(\lambda)}E(x,y,\lambda)$$

m: melanin, h: hemoglobin (1)

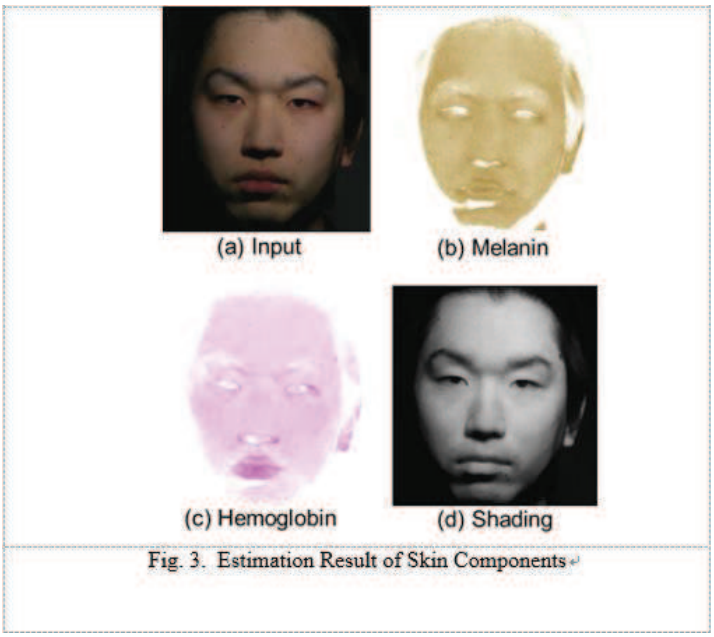

Fig. 3. Estimation Result of Skin Components

where $E(x,y,\lambda)$ denotes the spectral irradiance of incident light at point (x,y), $\rho_m(x,y)$, $\rho_h(x,y)$ denote the concentration of melanin and hemoglobin chromophore, $\sigma_m(\lambda)$, $\sigma_h(\lambda)$ denote absorption cross section of melanin and hemoglobin respectively, and $l_e(\lambda)$, $l_d(\lambda)$ denote light path in the epidermis and dermis layers. By putting polarization filters in front of the illumination and camera, we ignore the surface reflection. RGB signal on the position (x,y)in the image captured by the camera, $v_i(x,y), i = R,G,B$, can be modeled as

$$v_i(x,y) = k\int L(x,y,\lambda)s_i(\lambda)d\lambda = k\int e^{-\rho_m(x,y)\sigma_m(\lambda)l_e(\lambda)-\rho_h(x,y)\sigma_h(\lambda)l_d(\lambda)}E(x,y,\lambda)s_i(\lambda)d\lambda \quad (2)$$

where $s_i(\lambda)$denotes the spectral sensitivity of a camera, k denotes coefficient of camera gain. Spectral reflectance of skin is stable and it is roughly correlated with camera sensitivity. We approximately assume $s_i(\lambda) = \delta(\lambda - \lambda_i)$.

We assume spectral irradiance of incident light $\bar{E}(\lambda)$ is uniform over the observation area, and the shading coefficient $p(x,y)$ is accounts for the concavity and convexity of the surface. We derive

$$E(x,y,\lambda) = p(x,y)\bar{E}(\lambda) \quad (3)$$

Camera signal $v_i(x,y)$ can be simply rewrite as

$$v_i(x,y) = ke^{-\rho_m(x,y)\sigma_m(\lambda_i)l_e(\lambda_i)-\rho_h(x,y)\sigma_h(\lambda_i)l_d(\lambda_i)}p(x,y)\bar{E}(\lambda_i) \quad (4)$$

By taking the logarithm of both sides of Equation (4), we derive

$$\boldsymbol{v}^{log}(x,y) = -\boldsymbol{\rho}_m(x,y)\boldsymbol{\sigma}_m - \boldsymbol{\rho}_h(x,y)\boldsymbol{\sigma}_h + p^{log}(x,y)\mathbf{1} + \boldsymbol{e}^{\boldsymbol{log}} \quad (5)$$

where

$$\boldsymbol{v}^{log}(x,y) = [logv_R(x,y) \quad logv_G(x,y) \quad logv_B(x,y)]^T,$$
$$\boldsymbol{\sigma}_m = [\sigma_m(\lambda_R)l_e(\lambda_R) \quad \sigma_m(\lambda_G)l_e(\lambda_G) \quad \sigma_m(\lambda_B)l_e(\lambda_B)]^T,$$
$$\boldsymbol{\sigma}_h = [\sigma_h(\lambda_R)l_d(\lambda_R) \quad \sigma_h(\lambda_G)l_d(\lambda_G) \quad \sigma_h(\lambda_B)l_d(\lambda_B)]^T,$$
$$\mathbf{1} = [1 \quad 1 \quad 1]^T,$$
$$p^{log}(x,y) = \log(p(x,y)) + \log(k))$$
$$\boldsymbol{e}^{\boldsymbol{log}}(x,y) = [logE_R(\lambda_R) \quad logE_G(\lambda_G) \quad logE_B(\lambda_B)]^T \quad (6)$$

Figure 2 shows the relation of the input RGB signal and each component. The logarithm of the captured RGB signals $\boldsymbol{v}^{\boldsymbol{log}}$ can be represented by the weighted linear combination of the four vectors, $\boldsymbol{\sigma}_m$, $\boldsymbol{\sigma}_h$, shading vector $\mathbf{1}$ and the bias vector $\boldsymbol{e}^{\boldsymbol{log}}$. We predefine a skin color plane using training data set. The logarithm of the captured RGB signals $\boldsymbol{v}^{log}$ is projected onto the skin color plane along with the shading vector $\mathbf{1}$. From the position on the skin plane, we obtain the hemoglobin vector. Figure 3 shows an example of the result of melanin, hemoglobin, and shading components.

Ⅲ. Setup for BVP and PTT Measurement

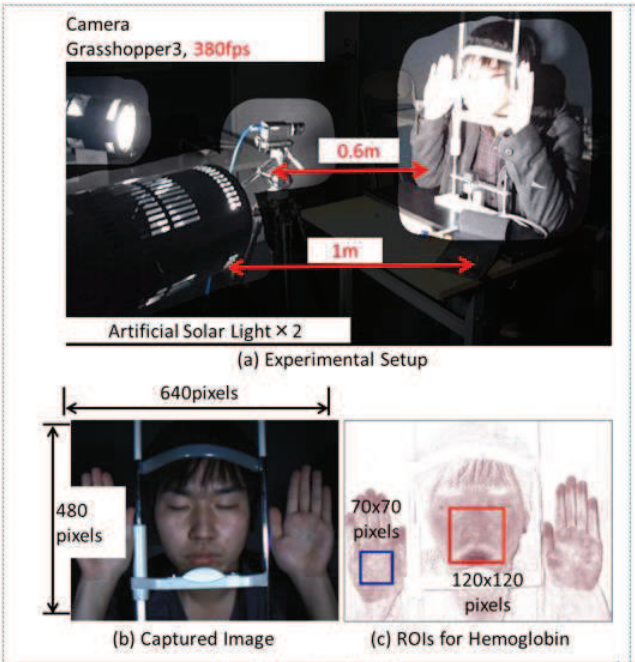

Fig. 4. Experimental Setup

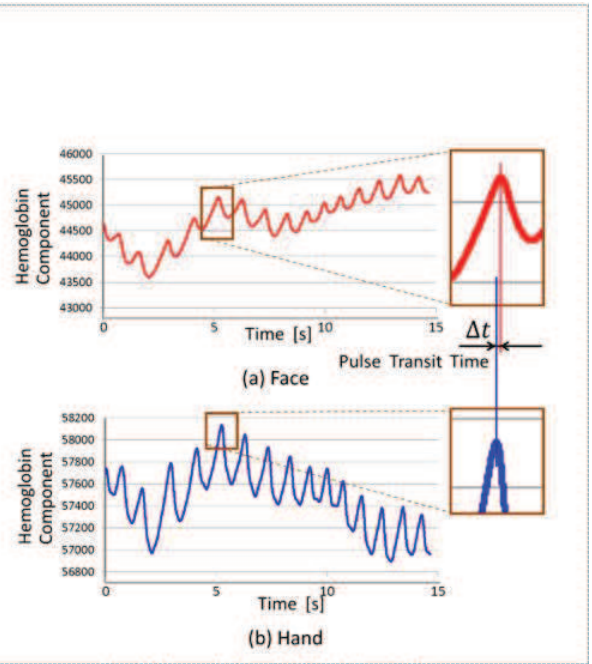

Fig. 5. Example Result of Pulse Transit Time

Figure 4 shows an experimental setup. We captured the video movies of the subject's face and hands at distance of 1 meter using a Point Grey Grashopper3 (GS3-U3-23S6C) camera. The illumination was an artificial solar light (SOLAX XC-100) at distance of 0.6 meters. All videos were recorded in color (30-bit

RGB with 3 channels × 10 bits/channel) at 380 frames per second (fps) with pixel resolution of 640 × 480 and saved in AVI format on the laptop. Figure 4(b) shows the example of a captured frame of the experimental data. The subject put his head on chin-rest and forehead-rest, in order to keep the subject as still as possible. Using each fr

we estimate the amount of hemoglobin component with the method of Section 2 as shown in Figure 4(c). We set measurement region (ROI) on the face, right hand with pixel sizes of 120 × 120 pixels and 70 × 70 pixels respectively. We calculated the average value of the

hemoglobin component in each ROI.

Figure 5 show the example result of the temporal change of the hemoglobin component in the face region and in the right hand region respectively. Each wave has 15 peaks in 15 seconds. You can see the difference of the peak time differences between the each hemoglobin component behaviors. The time gap indicate pulse transit time (PTT). In our experiment, we detect peak timing using the frame number which has peak value of hemoglobin component and convert the frame number into time domain by the conversion with frame rate.

Ⅳ. Experimental Results

In this section, we first explain the experimental procedure and show the experimental results. The purpose of the experiment is to check the feasibility of our PTT evaluation method. For the purpose, we measured PTT with the proposed method described in section 3 and also measured the blood pressure using conventional sphygmomanometer (OMRON HEM-7132) for ground truth. And we evaluated the correlation between PTT by the proposed method and the ground truth. In order to evaluate a wide variety of blood pressures, we asked each subjects to do a squat exercise before capturing video, capture video and measure ground truth. We did this procedure repeatedly for each subject. We evaluate blood pressure using systolic pressure, which indicate maximum blood pressure, and a mean arterial pressure (MAP), which is the average over a cardiac cycle. MAP can be approximately determined from measurements of the systolic pressure P_{sys} and the diastolic pressure P_{dias} as following

$$MAP \cong P_{dias} + (P_{sys} - P_{dias})/3 \quad (7)$$

Experimental results are shown in Figures 6 and 7. Figure 6 shows the relation between PTT and systolic pressure. We evaluated three subjects. The horizontal axis of

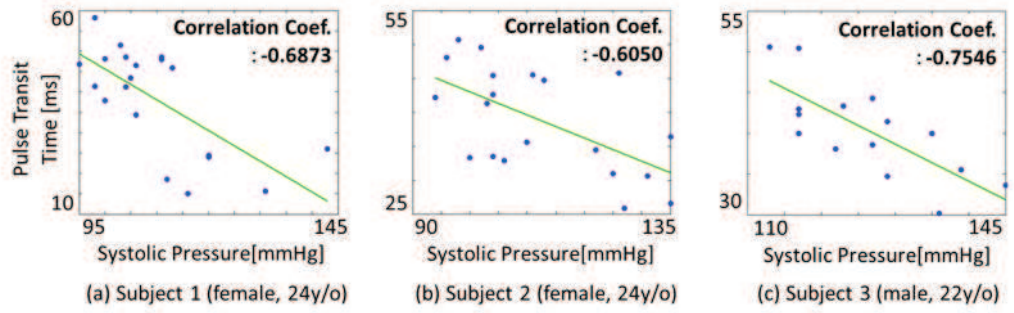

Fig. 6. Relation between Pulse Transit Time and Systolic Pressure

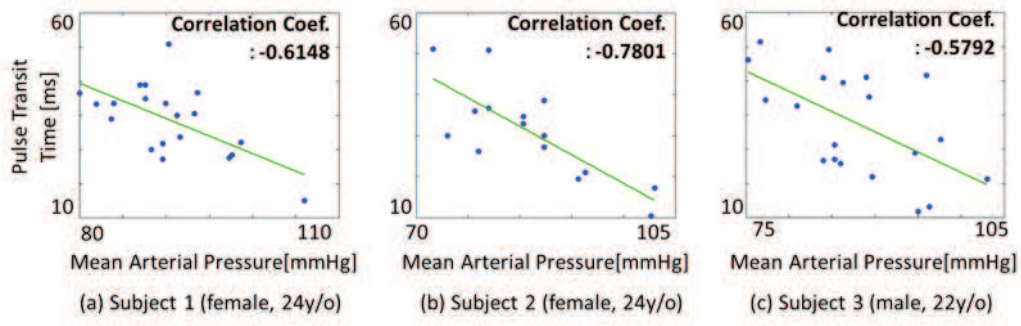

Fig. 7. Relation between Pulse Transit Time and Mean Arterial Pressure. (Subject 1, 2 and 3 are all Asian.)

each graph shows systolic pressure P_{sys} and the vertical axis indicates PTT. The blue dot in each graph shows a measurement. Each data have several dots since we measure PTT and blood pressure repeatedly for each subject. The correlation coefficient between PTT and systolic pressure are -0.6873, -0.6050 and -0.7546 respectively.

Figure 7 shows the relation between PTT and mean arterial pressure (MAP). The correlation between PTT and MAP are -0.6148, -0.7801 and -0.5792 respectively. The results show some variation of correlation coefficient due to the subjects. The one of the reasons comes from the experimental condition. In this experiment, blood pressure as ground truth was measured after capturing movie for PTT. There were certain time gap and it changed in each experiment.

As a prior art, Sugita at el. [12] evaluated the relation between PTT and blood pressure using contact device and confirmed the correlation coefficient -0.658 (The correlation coefficient is written as 0.658 in the paper originally). Kato at el. [13] also evaluated it using contact device and confirmed the correlation -0.848 using contact device. Hence our result of correlation coefficient also showed strong correlation coefficient between PTT and blood pressure and it is almost same as the result of the prior arts, even though our results was obtained by non-contact measurement whereas the prior arts obtain the results using contact measurement.

We also evaluated BVP measurements at several body parts as shown in Figure 8: bottom of foot, chest, top of foot and back of foot.

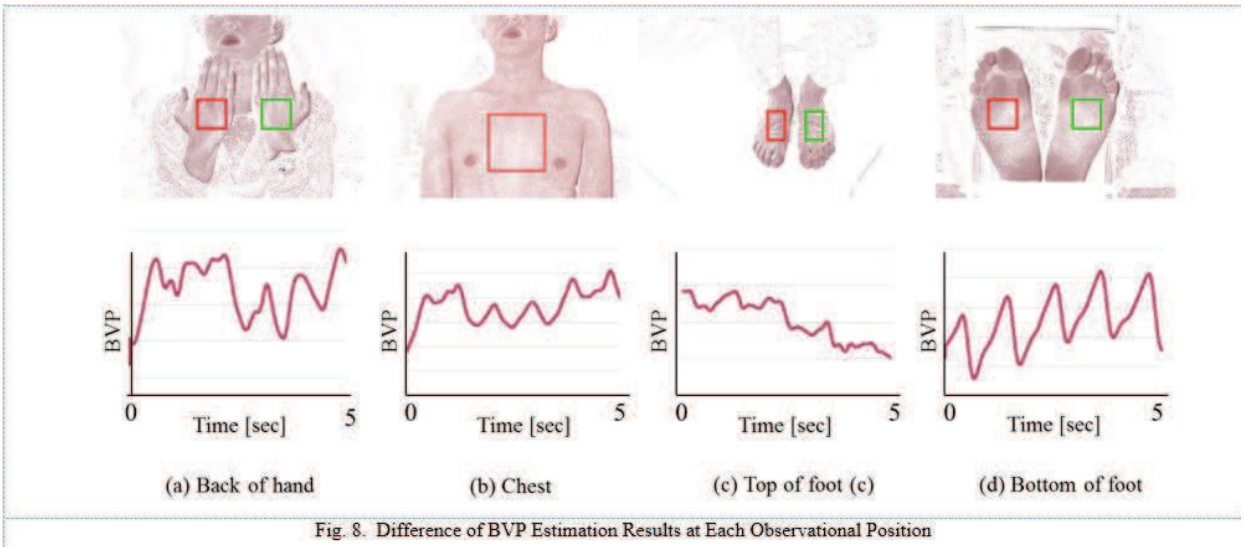

Fig. 8. Difference of BVP Estimation Results at Each Observational Position

The back of foot showed clear BVP wave. On the other hand, others did not show clear BVP wave. This result indicates that the selection of suitable measurement position is also important for our remote PTT measurement. The difference may be caused by the difference in skin thickness. This is a research subject for future work.

In our experiment, the number of the subjects is limited. We have to evaluate more subject in order to evaluate statistically significant differences. It is for future work.

Ⅴ. CONCLUSION

We proposed a non-contact video based estimation method of pulse transit time (PTT) using the quantitation method of hemoglobin composition. The proposed method can measure PTT only by using video data which is captured remotely. It is very effective and it has potential to improve the usability of blood pressure measurement.

We also evaluated the correlation between PTT measured by the proposed method and blood pressure measured by a sphygmomanometer cuff. As a result, we achieved high correlation between -0.5792 and -0.7801, which confirms the effectiveness of the proposed method.

We acknowledge that there are several limitations in this study. In this paper, we only evaluated Asian subjects. We have to confirm the effectiveness for Caucasian and Negroid subjects as well. Number of the subjects is also limited. We will evaluate more subjects for future work. There is much room for the improvement of the experimanrtal setup. In our expriment, there were certain time gap between captureing video for the experimental data of PTT and blood pressure for grand truth. By using continuous sphygmomanometer, we can eliminate the time gap. The improvement of the hemoglobin estimation model might be effective to improve the stability and accuracy of the PTT measurement.

REFERENCES

[1] Fortuna EL, Carney MM, Macy M, Stanley RM, Younger JG, Bradin SA. Accuracy of non-contact infrared thermometry versus rectal thermometry in young children evaluated in the emergency department for fever. J Emerg Nurs. Mar 2010;36(2):101-104.(2010)

[2] Chiappini E, Sollai S, Longhi R, et al. Performance of non-contact infrared thermometer for detecting febrile children in hospital and ambulatory settings. J Clin Nurs. May 2011;20(9-10):1311-1318. (2011)

[3] Non-Contact Thermometers for Detecting Fever: A Review of Clinical Effectiveness. Ottawa ON: 2014 Canadian Agency for Drugs and Technologies in Health. (2014)

[4] H. Aoki et al., “Non-contact Respiration Measurement Using Structured Light 3-D Sensor,” in SICE, 2012, pp. 614–618.(2012)

[5] M.-Z. Poh, D. J. McDuff, and R. W. Picard, “Non-contact, automated cardiac pulse measurements using video imaging and blind source separation,” Optics Express, vol. 18, no. 10, pp. 10 762–10 774, (2010).

[6] D. McDuff, S, Gontarek, R. W. Picard, "Improvements in Remote Cardio-Pulmonary Measurement Using a Five Band Digital Camera" IEEE Transactions on Biomedical Engineering, pp. 2593-2601, (2014).

[7] http://www.healthcare.omron.co.jp/corp/news/2016/0105.html

[8] D. Shao, Y. Yang, C. Liu, F. Tsow, H. Yu and N. Tao, "Noncontact Monitoring Breathing Pattern, Exhalation Flow Rate and Pulse Transit Time", IEEE Trans. Biomed. Eng., vol.61, no.11, pp.2760-2767, Nov., (2014)

[9] K.Murakami, M. Yoshiola, J. Ozawa, "Non-contact Pulse Transit Time Measurement using Imaging Camera, and its Relation to Blood Pressure",14th IAPR International Conference on Machine Vision Applications (MVA), May (2015)

[10] N. Tsumura, N. Ojima, K. Sato, "Image-based skin color and texture analysis/synthesis by extracting hemoglobin and melanin information in the skin,” ACM Transactions on Graphics, Vol.22, No.3, 770-779, (2003).

[11] Hiraoka M., Firbank M., Essenpreis M., Cope M., Arridge S. R., van der Zee P. and Delpy D. T., "A Monte Carlo investigation of optical pathlength in inhomogeneous tissue and its application to near-infrared spectroscopy", Phys. Med. Biol. 38 1859–76 (1993)

[12] N. Sugita, M. Yoshizawa, A. Tanaka, T. Masuda, K. Abe, T. Yambe, S. Nitta, "Evaluation of Biological Effects of Visual Stimulation Based on a Portable Measuring Device for Blood Pressure and Heart Rate", SICE Conference, pp.2030-2033, Aug.4-6th (2003)

[13] Y. Kato, M. Nambu, M. Imura, Y. Kuroda, O. Oshiro,"Smart Sensing of Cardiovascular Physiological Information from Soles without Direct Skin Contact",34th Conf. IEEE EMBS, pp.5806-5809 Aug.28-Sep.1 (2012)

Munenori Fukunishi received B.S. and M.S. degree in mechanical engineering from Waseda University, Japan, in 1999 and Tokyo Institute of Technology, Japan, in 2001 respectively. After having professional research career at Hitachi Ltd. and Keyence Corp., he joined Olympus Corporation in 2007. He has been engaged in research on image processing algorithm for medical and industrial endoscope. From 2013 to 2014, he was a visiting scholar at Stanford University. He is now a student of PhD course for working individuals at Chiba University. His research interests include image quality evaluation and color filter array study, 3D reconstruction, medical and healthcare application.

Taku Yonezawa received B.S. and M.S. degree in informatics and imaging systems from Chiba University in 2014 and 2016 respectively. In 2016, he joined NTT DOCOMO Inc., the largest telecommunications company in Japan.

Genki Okada received B.S. degree in informatics and imaging systems from Chiba University in 2016. He is now a student of M.S. course degree at Chiba University. His research interests include remote observation of vital signs and affective computing.

Kouki Kurita received B.S. and M.S. degree in informatics and imaging systems from Chiba University in 2015 and 2017 respectively. In 2017, he joined Fujitsu Corporation, Japan.

Shoji Yamamoto received his B.E. and M.E. degrees from the Department of Opt-Electro-Mechanics Engineering from Shizuoka University in 1989 and 1991 respectively. From 1992 to 2007, he worked Mitsubishi Heavy Industries, Information and Electronics Research Center in Japan. And he received Dr. Eng degrees in information science from Chiba University in 2007. He is currently Professor in Tokyo Metropolitan College of Industrial Technology, Japan. He is interested in Vision science, Image processing, and Computer graphics. He is a member of the Optical Society of Japan, the Institute of Image Information and Television Engineers, and the Institute of Image Electronics Engineers of Japan.

Norimichi Tsumura was born in Wakayama, Japan, on 3 April 1967. He received the B.E., M.E. and Dr. Eng degrees in applied physics from Osaka University in 1990, 1992 and 1995, respectively. He moved to the Department of Information and Computer Sciences, Chiba University in April 1995, as an assistant professor. He was a visiting scientist in University of Rochester from March 1999 to January 2000. He is currently associate professor in Department of Information and Image Sciences, Chiba University since February 2002, also was a researcher in PRESTO, Japan Science and Technology Corporation (JST) from December 2001 November 2005. He got the Optics Prize for Young Scientists (The Optical Society of Japan) in 1995, Applied Optics Prize for the excellent research and presentation (The Japan Society of Applied Optics) in 2000, Charles E. Ives Award (Journal Award: IS&T) in 2002. He is interested in the color image processing, computer vision, computer graphics and biomedical optics